

Devices and Methods for Rapid 3D Photo-Capture and Photogrammetry of Small Reptiles and Amphibians in the Laboratory and the Field

Because of the importance of specimen identification, and for establishing protocols for new species boundaries, novel methods and tools for identifying and sharing specimen data for vertebrate organisms, particularly amphibians and reptiles, is an important aim for taxonomists (Dayrat 2005; McDiarmid et al. 2011). In general, the gold standard for specimen collection and identification for reptiles and amphibians is euthanization with appropriate preservation and deposition as vouchered material in natural history holdings (Allmon 1994; Davis 1996; Shaffer et al. 1998; Suarez and Tsutsui 2004; Reynolds and McDiarmid 2011; Simmons 2015). This important approach will rightfully remain the gold standard for collecting and identifying most reptile and amphibian specimens (McDiarmid et al. 2011). However, there is also value in establishing other methods to gain specimen identification as a complement to this method. Several methods already exist (Simmons 2015), including photographs, audio recordings, and scientific illustrations, among others (e.g., <https://soundcloud.com/frogvoicesofborneo>).

Photographs have proven to be a useful resource for specimen identification and are widely used in online resources such as AmphibiaWeb (amphibiaweb.org). The collection of audio recordings is especially valuable for recording of vocalizations, such as from frogs (e.g., Köhler et al. 2017). Scientific illustrations can be a valuable tool for effective recreation of specimens, especially for emphasizing key elements of scalation and color that might be challenging to document in a photograph. Here, we describe novel tools and techniques for the creation of 3D models of live reptiles and amphibians, both in wild settings in the field and in the laboratory.

Over the last few years, there has been increasing interest in establishing 3D techniques to describe various kinds of specimens, with a focus on museum specimens such as bones, skulls, or other physical features (Aldridge et al. 2005; Chiari et al. 2008; Falkingham 2012; Boyer et al. 2015; Evin et al. 2016; Gignac et al. 2016; Bot and Irschick 2019). The value of 3D scanning methods is their ability to represent high-quality, accurate, shareable, and (typically) complete 3D visualizations of the specimen. Methods for 3D reconstruction include 3D photogrammetry, laser and white-light scanning, and CT-scanning, among others (Weinberg et al. 2004; Gunga et al. 2007; Falkingham 2012; Laforsch et al. 2012). Although widely used for preserved museum specimens, explanation of how these methods can be used for live specimens in the field or the laboratory has been largely unexplored, with some exceptions (Bot and Irschick 2019; Irschick et al. 2020b). However, these methods hold great potential for identifying and cataloguing live reptile and amphibian specimens. This is especially timely given the increasing restrictions placed on scientists striving to access and export reptile or amphibian specimens (Renner et al., 2012). In addition, the software, hardware, and methods for creating and visualizing 3D data have been rapidly evolving over the past decade, and thus represent new opportunities as a powerful visualization tool for specimens.

Here, we present novel inexpensive, portable, multi-camera 3D photogrammetry devices that can relatively quickly (1–2 min) create accurate 3D models of live reptile and amphibian species, either in field or laboratory settings. Further processing (several hours) of computer processing time can then result in high-quality RAW 3D models. Finally, an additional input of time (multiple hours) by CG artists can result in full-body 3D meshes for these specimens. 3D photogrammetry is a proven method for accurate recreation of both the shapes and colors of objects using photographs, but while this method is widely used in forensics, art history, paleontology and archaeology, and other scientific applications (Weinberg et al. 2004; Falkingham 2012; Evin et al. 2016), its usage for live animals, including reptiles and amphibians, has hardly been documented (but see Bot and Irschick 2019). We describe the construction of these devices, their usage, and describe the basic workflow of 3D photogrammetry for small reptiles and

DUNCAN J. IRSCHICK*

*Department of Biology, 221 Morrill Science Center,
University of Massachusetts, Amherst, Massachusetts 01003, USA*

ZACHARY CORRIVEAU

*Department of Biology, 221 Morrill Science Center,
University of Massachusetts, Amherst, Massachusetts 01003, USA*

TREVOR MAYHAN

*Department of Biology, 221 Morrill Science Center,
University of Massachusetts, Amherst, Massachusetts 01003, USA*

CAMERON SILER

*Sam Noble Oklahoma Museum of Natural History and
Department of Biology, University of Oklahoma,
2401 Chautauqua Avenue, Norman, Oklahoma 73072-7029, USA*

MARK MANDICA

*Amphibian Foundation, 4055 Roswell Rd NE, Atlanta,
Georgia 30342, USA*

TONY GAMBLE

*Marquette University, Wehr Life Sciences 109, 1428 W. Clybourn
Street, Milwaukee, Wisconsin 53233, USA
Milwaukee Public Museum, 800 W. Wells Street, Milwaukee,
Wisconsin 53233, USA*

*Bell Museum of Natural History, University of Minnesota,
1987 Upper Buford Circle, St. Paul, Minnesota 551088, USA*

JOHNSON MARTIN

2111 High Street, Wilmore, Kentucky 40390, USA

JER BOT

<http://verbal007.com/>

SAVVAS ZOTOS

*Terra Cypria—the Cyprus Conservation Foundation, Agiou Andreou 341,
3035, Limassol, Cyprus
School of Pure and Applied Sciences, Open University of Cyprus,
PO Box 12794, 2252, Nicosia, Cyprus*

**Corresponding author; e-mail: irschick@bio.umass.edu*

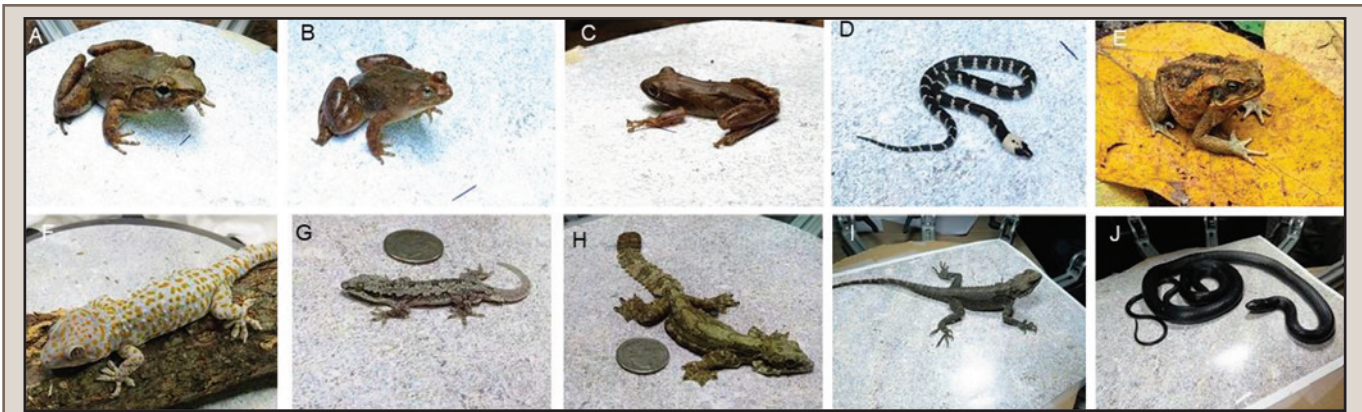


FIG. 1. The 10 species used in this 3D photogrammetry study. From left to right, top to bottom, the specimens are: *Limnonectes macrocephalus*, *Occidozyga laevis*, *Polypedates leucomystax*, *Lycodon capucinus*, *Rhinella marina*, *Gekko gekko*, *Hemidactylus platyurus*, *Gekko kuhli*, *Stellagama stellio cypriaca*, and *Dolichophis jugularis cypriacus*.

TABLE 1. Reptile and amphibian specimens captured for the 3D analysis. SVL is in cm. ID numbers are OMNH (Oklahoma Museum of Natural History).

Species	Locality	SVL	Type	Museum ID	Link
<i>Limnonectes macrocephalus</i>	Philippines	9.8	RAW scan	47709	https://skfb.ly/6EslS
<i>Lycodon capucinus</i>	Philippines	13.2	RAW scan	4654	https://skfb.ly/6sCQM
<i>Occidozyga laevis</i>	Philippines	5.0	RAW scan	47728	https://skfb.ly/6ROpu
<i>Polypedates leucomystax</i>	Philippines	5.3	RAW scan	47785	https://skfb.ly/6ROpZ
<i>Rhinella marina</i>	Philippines	9.9	RAW scan (leaf)	46722	https://skfb.ly/TyOR
<i>Gekko gekko</i>	Captive	14.4	RAW scan (branch)		https://skfb.ly/VLpB
<i>Hemidactylus platyurus</i>	Captive	5.3	Full-body 3D mesh		https://skfb.ly/6ROpX
<i>Gekko kuhli</i>	Captive	8.5	Full-body 3D mesh		https://skfb.ly/6ROpW
<i>Gekko gekko</i>	Captive	14.4	Full-body 3D mesh		https://skfb.ly/6SNEn
<i>Stellagama stellio cypriaca</i>	Cyprus	10.7	Full-body 3D mesh		https://skfb.ly/6ROpL
<i>Dolichophis jugularis cypriacus</i>	Cyprus	146.0	Full-body 3D mesh		https://skfb.ly/6RMRn

amphibians both in the field and in the lab. We demonstrate this process by providing examples with 10 species total (four frog species, four lizard species, and two snake species), with five specimens (four frogs, one snake) photocaptured in the field, and five in the laboratory. From these 10 species, we created a total of 11 3D models of which six were RAW (unprocessed) scans, and five were complete (full-body) 3D meshes re-created by CG artists (one species was presented both as a RAW and full-body 3D mesh). By RAW, we mean scans which have not been significantly edited by CG artists and represent initial 3D output. The full-body 3D meshes only show body shape, and not the colors and textures of the species. We demonstrate the relative accuracy of our approach by comparing measurements taken on live individuals with that taken on the digital specimens.

METHODS

Specimens.—Table 1 lists all ten species and 11 models (one model was provided both in RAW and full-body format to demonstrate the transition) and an appropriate size metric (Fig. 1). All specimens were adults, with the exception of the *Lycodon* snake, which was a subadult. The specimens came from three sources: 1) Field specimens from two separate trips to the Philippines in 2016 (*Rhinella marina*) and 2017

(*Limnonectes macrocephalus*, *Lycodon capucinus*, *Occidozyga laevis*, *Polypedates leucomystax*); 2) captive specimens from the Irschick Laboratory at the University of Massachusetts at Amherst (*Gekko gekko*, *G. kuhli*, *Hemidactylus platyurus*); and 3) field specimens from the Zotos Laboratory at the Terra Cypria Foundation in Cyprus (*Dolichophis jugularis cypriacus*, *Stellagama stellio cypriaca*). Of the above specimens, the specimens from the Philippines were all deposited as museum specimens at the Sam Noble Oklahoma Museum of Natural History (OMNH): *Limnonectes macrocephalus* (OMNH 47709), *Lycodon capucinus* (OMNH 46546), *Occidozyga laevis* (OMNH 47728), *Polypedates leucomystax* (OMNH 47785), and *Rhinella marina* (OMNH 46722).

Specimens were collected from five field sites: 1) 2016 – Philippines, Luzon Island, Camarines Norte Province, Tulay na Lupa (*Rhinella marina*); 2) 2017 – Philippines, Luzon Island, Cagayan Province, Nasipping, Nasipping Reforestation Project (*Polypedates leucomystax*); and 3) 2017 – Philippines, Luzon Island, Nueva Vizcaya Province, Maddiangat, Mt. Palali, (*Limnonectes macrocephalus*, *Lycodon capucinus*, and *Occidozyga laevis*). 4) 2019 - Cyprus, Limassol district, near Kolossi village (*Dolichophis jugularis cypriacus*); 5) 2019 - Cyprus, Limassol district, near Parekklesia village (*Stellagama stellio cypriaca*). Additional information on some of the specimens can be obtained through consulting the Oklahoma

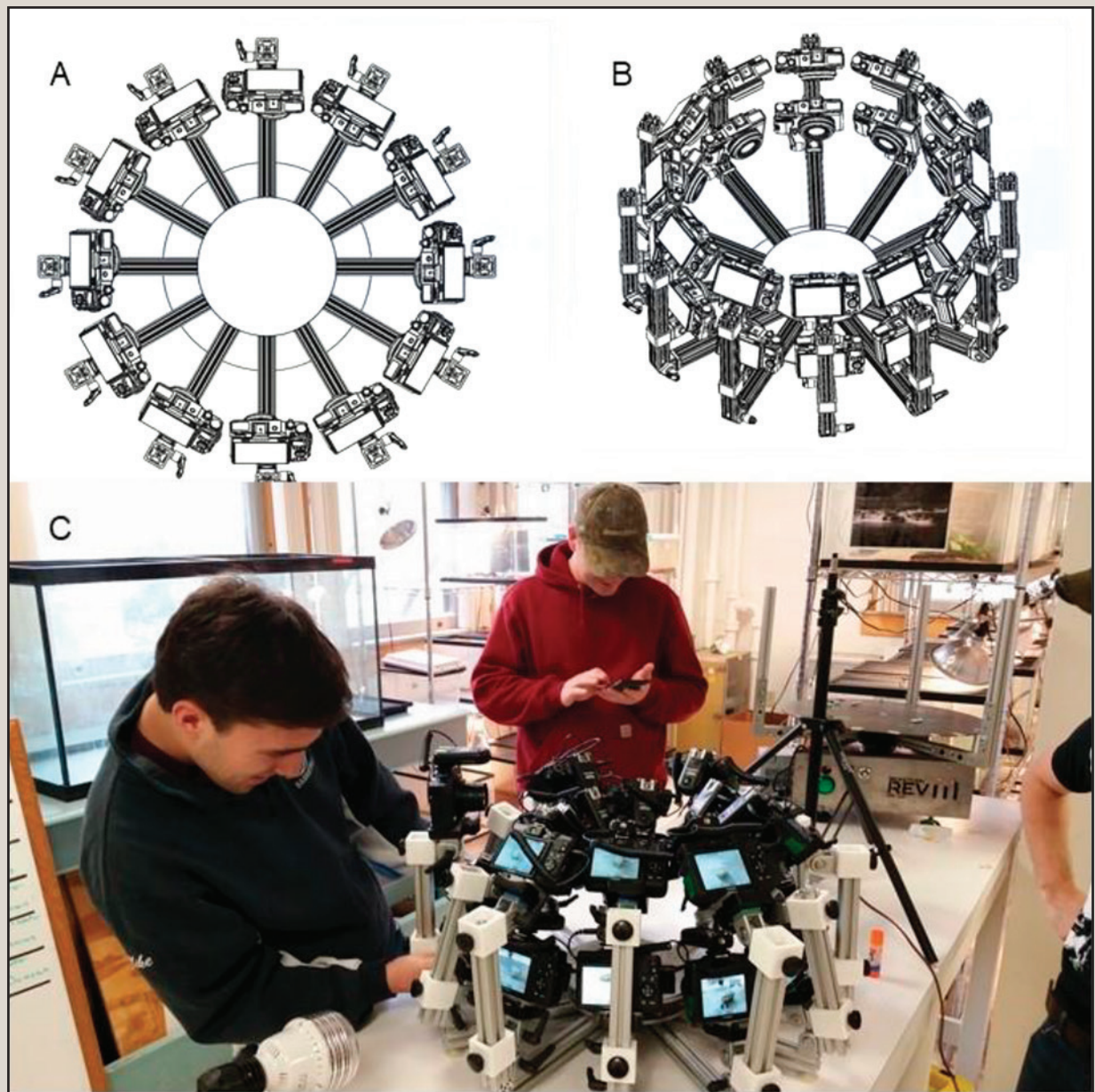


FIG. 2. The 12-armed MACRO multi-camera rig, which is designed for smaller organisms of between about 2 and 20 cm in length. Panel A shows the top view and Panel B shows a side view. Panel C shows the MACRO in use at the University of Massachusetts at Amherst.

Museum of Natural History website through their OMNH numbers in Table 1. The Cyprus specimens were released several days after capture at their original collection points. The Irschick captive laboratory specimens were all obtained originally through the commercial pet trade.

3D photogrammetry methods.—We created two custom devices to photo-capture small reptiles and amphibians both in the field and in the laboratory. We term these devices the MACRO (Fig. 2) and ARRAY systems (Fig. 3). The MACRO system uses a circular array of up to 24 small digital cameras on 12 foldable arms and a stationary center plate to obtain 3D models of small organisms ranging from about 2.5 to 22 cm in length (total width of device is 61 cm). The close configuration of the cameras enables them to be used with macro settings, which are ideal for photography of smaller specimens. The system is rotatable, and provided the subject has not moved,

the camera arms can be moved to gain additional photos, which can be repeated as necessary to gain sufficient images for reconstruction. The MACRO arms can be folded inwards to fit into a carrying case and can then be redeployed with no assembly required.

The ARRAY system is like the MACRO device, except being larger, and therefore is best suited for organisms ranging from about 22 cm to 35 cm in length, although a larger snake or lizard that is curled could also be scanned. The ARRAY is also rotatable, 97 cm in total diameter, with 15 fixed arms for cameras, and has a central plate which is 46 cm in diameter. The system, because of its larger size, can accommodate a larger number of cameras, such as three small Canon G16 cameras on each vertical arm or one on each horizontal brace (up to 60 cameras, although we typically used 30). Because of its larger size and weight, the ARRAY device is better suited to laboratory research on larger

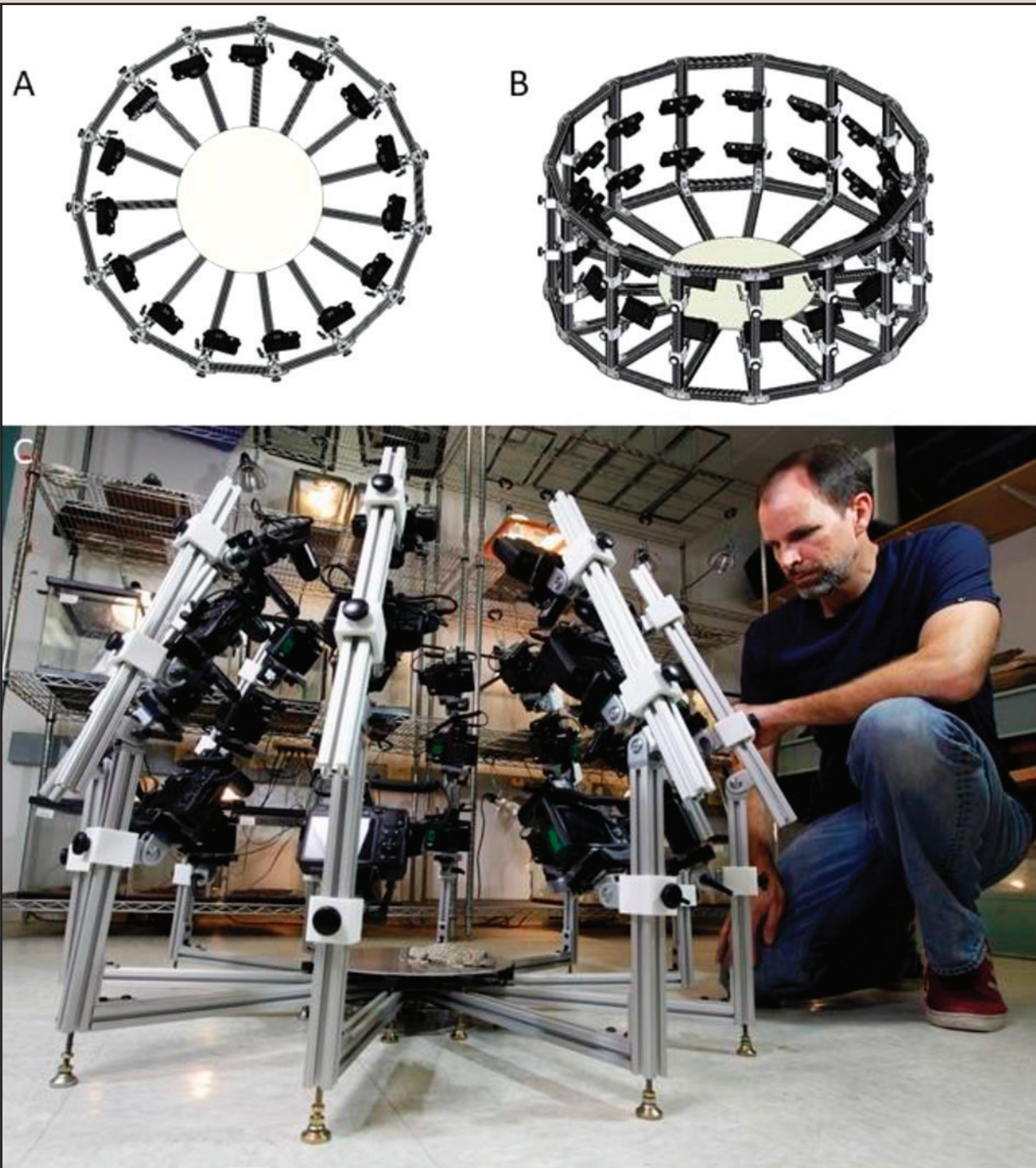


FIG. 3. The 15-armed ARRAY multi-camera rig, which is designed for smaller to mid-sized organisms ranging from about 20 to 60 cm in length. Panel A shows the top view and Panel B shows a side view. Panel C shows the MACRO in use at the University of Massachusetts at Amherst.

specimens and is less amenable to being transported to remote field locations, although it can be disassembled and placed into a carrying case. Both devices were built using all off the shelf products, and each custom base plate was machined in the UMass Amherst Machine Shop. We used 12 MP Canon G16 cameras (Focal lengths 28–140 mm) with this system, which had wireless triggers (RF-603C II Remote Flash Trigger Kit from Yongnuo) set to the same channel so that the photographer could automatically trigger all the cameras simultaneously. For each of the photoshoots, we used 12 cameras for the MACRO and 30 for the ARRAY, although because of the rotational ability,

we were able to capture between about 24 to about 90 images per specimen. We used either ambient light (all research in the Philippines, see below), or 250W 125V LED bulbs on stands for external lighting for modelling (all other models). Only the *Gekko gekko* was scanned with the ARRAY device. *Rhinella* was photographed with a CANON Mark III camera and a 100mm lens while walking around it. The other specimens were all scanned using the MACRO device.

Underside images and other assorted images.—Beside 3D scanning the live animals using the MACRO or ARRAY devices, several close-up pictures of the animals were taken using

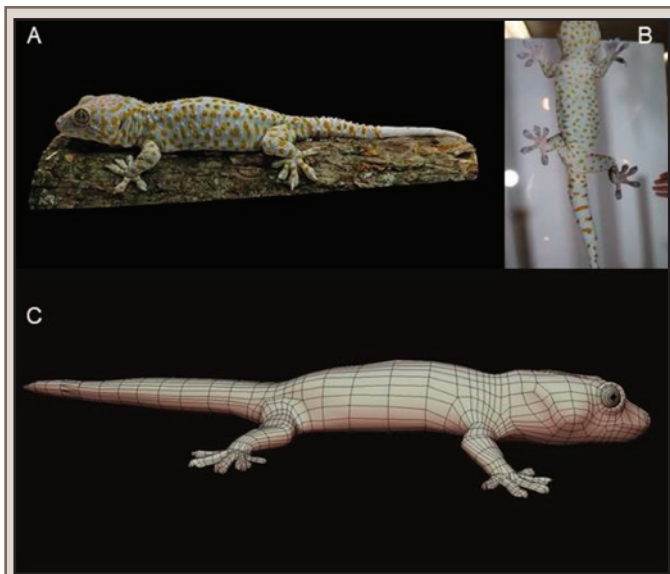


FIG. 4. Three images which show how a single 3D model can be reconstructed from scans and photos taken from individual reptiles. The key elements include a 3D scan of the dorsal side of an animal (A, Tokay Gecko, *Gekko gekko*), photocaptured with the ARRAY camera rig, images of the underside of the animal, as well as other more obscure areas of the body (B), resulting in the final 3D mesh (C) which incorporates both the 3D scan, images, and measurements to ensure accuracy.

Canon G16 or the CANON Mark III cameras (the latter had a 100 mm MACRO lens). Through those pictures, we aimed to document features or/and parts of the animals that were unique or more challenging to visualize in the 3D scan. These images also represented another source of high-quality data for the CG artists to accurately represent those features. The ventral surface was typically visualized through photographing the specimens when they were resting on a clean glass plate.

3D model reconstruction.—We created two kinds of models. One set of models were RAW models, which represent 3D photogrammetry scan output from Capturing Reality Software, and which were not retopologized, or were altered. These tend to be large (> 50 MB) files with a great level of texture and detail, and typically a large (> 1 million) number of vertices. For these RAW models, these specimens were photoscanned when sitting in a typical “neutral” pose (i.e., a frog sitting in a typical “tucked” position, lizards with all four limbs placed outwards, and snakes with their bodies spread out) on a surface, such as a piece of paper, or a more natural substrate (e.g., a leaf or branch). The other kind of model were 3D mesh models, which were full body reconstructions of specimens. These reconstructions were based on RAW scans, as well as photographs and measurements of the original specimen, and follow the detailed protocol laid out in Bot and Irschick (2019). We briefly explain this procedure below.

For the full-body 3D meshes, we worked with two CG artists who reconstructed them using methods outlined in Bot and Irschick (2019). The team members work together as part of the Digital Life Project (www.digitallife3d.org) and share a set of techniques that provide a level of consistency among the models. This workflow is briefly summarized here. Our process began with using a high-quality 3D scan of the dorsal view of the specimen using Capturing Reality Software (<https://www.capturingreality.com/>), Meshroom (Alicevision 2018)

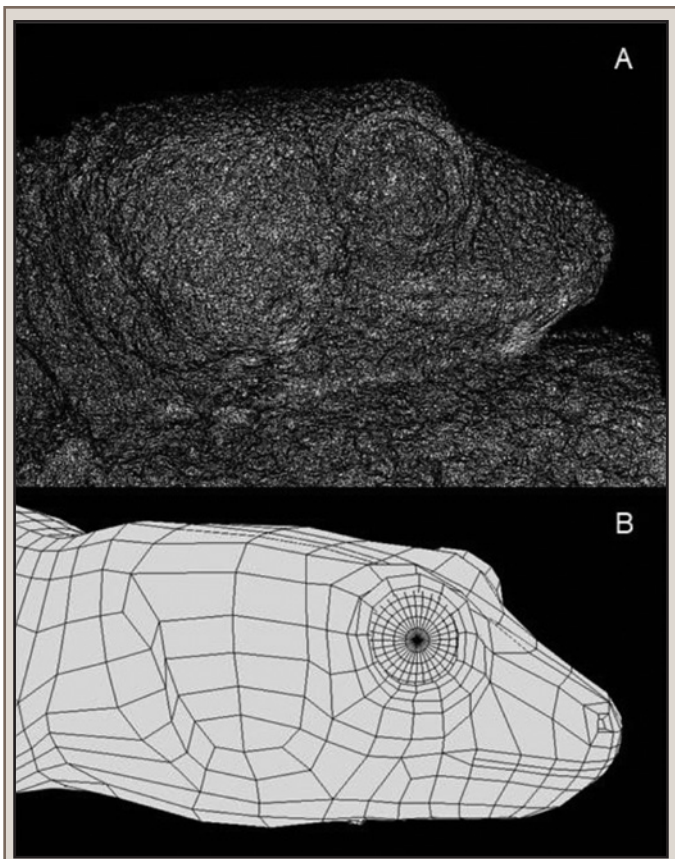


FIG. 5. Panel A shows mesh topology from a RAW scan of a Tokay Gecko (*Gekko gekko*), whereas Panel B shows the retopologized version on the same individual as a full 3D model.

or Colmap (Schönberger and Frahm 2016), and then created single 3D models of each individual using Blender software (Community 2018). The undersides of the specimens for the full-body 3D meshes were created using the original RAW scan combined with images taken of the underside of specimens, as well as measurements (Fig. 4, Appendix 1). The surface of the RAW scans was projected onto a new retopologized base mesh to create the majority of the 3D models. We retopologized the models manually using Blender. However, the RAW scans lacked sufficient data for reconstruction of the ventral surfaces, so photo reference of the body underside was used to create the surface of the underside. Basic morphometric measurements were used to ensure that the photo reference and mesh were to the same scale. Once the surface was projected and the ventral surface manually reconstructed, any errors in the projection, such as surface noise, were sculpted to match the reference images of both the ventral and dorsal sides. One advantage of the full-body 3D meshes was the overall lower level of complexity in the 3D mesh, which reduced file size (Fig. 5). As an example of this reduction of size, the RAW scan of *Gekko gekko* had 2.2 million triangles, whereas the full 3D mesh model had 7.7 thousand triangles.

The terms “resolution” and “accuracy” within the context of 3D photogrammetry and 3D modelling require some brief explanation. It is challenging to assess “accuracy” at a very fine scale without sophisticated measurement devices. Determining accuracy on a larger measurement scale is more straightforward, such as comparing whether a digital measurement of a limb, for example, is similar to a physical

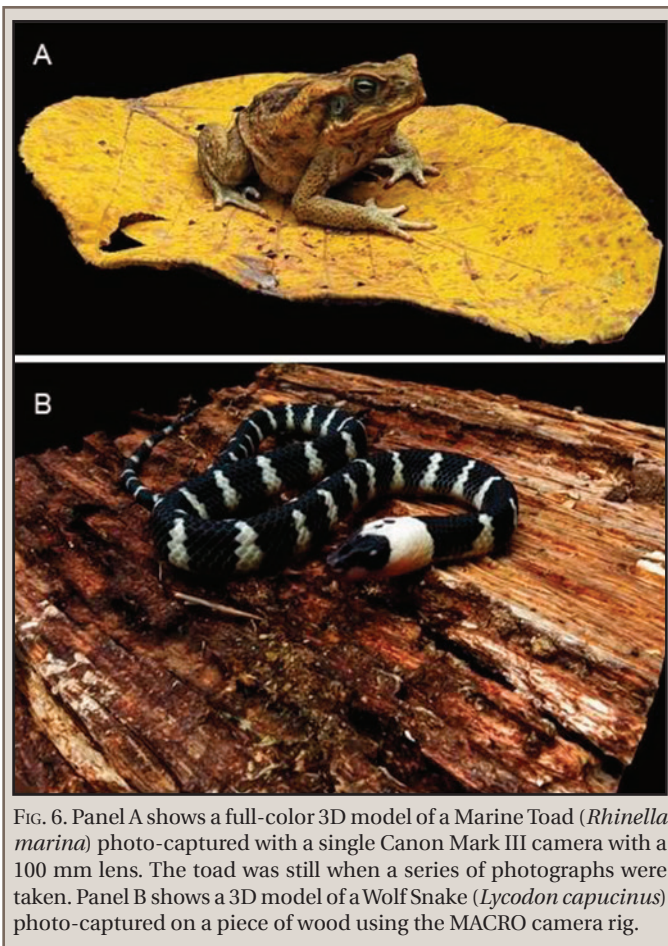


FIG. 6. Panel A shows a full-color 3D model of a Marine Toad (*Rhinella marina*) photo-captured with a single Canon Mark III camera with a 100 mm lens. The toad was still when a series of photographs were taken. Panel B shows a 3D model of a Wolf Snake (*Lycodon capucinus*) photo-captured on a piece of wood using the MACRO camera rig.

measurement of a limb. Here, we only refer to “accuracy” in this broader sense. A more relevant term is “resolution,” which refers to the level of detail that is effectively reconstructed by the scanning method. Unlike scanning methods such as CT-scanning and laser scanning, 3D photogrammetry does not automatically provide a set level of resolution (e.g., 0.1 mm, 1 mm). Indeed, resolution will vary according to several parameters discussed below, but at the high level, with certain imaging systems and conditions (and objects), accuracy has been reported as high as 0.1 mm by some companies (https://www.photodeler.com/kb/factors_affecting_accuracy_in_photogramm/), but this is rarely achievable for most scientific applications, as resolutions of about 1 mm (Tucci et al. 2001; González-Vera et al. 2020) are more typical. Quantifying level of resolution in any 3D photogrammetry study requires significant additional analysis that is beyond the scope of our study, but given that we were able to achieve a good depth of field due to the large size of the objects (small reptiles and amphibians), and because we employed other good practices (e.g., cameras on tripods, reasonable megapixel counts (12 MP), good lighting), a resolution of around 1 mm is a reasonable approximation.

Some of the factors affecting resolution include: 1) camera type and megapixel count. In general, cameras with a higher megapixel count (e.g., Canon 5DS, 50.6 megapixel) will enable higher levels of resolution, assuming basic good practices with photography, such as even, plentiful lighting. Similarly, higher-quality DSLRs with superior sensors will typically enable superior levels of resolution than lower-quality DSLRs

under similar conditions. 2) Filling the camera frame with the image is critical to achieving higher levels of resolution, especially in the context of megapixel count. For example, if an image of a sea turtle fills up 1/3 of a frame in a camera that has a $4K \times 3K$ resolution, then the overall resolution has the potential to be dropped by 2/3 or more. 3) Use of a tripod and achieving a higher depth of field (such as with higher aperture settings) will enable sharper images, which in turn will allow photogrammetry software to more effectively reconstruct the object. Other considerations in achieving higher levels of 3D photogrammetry resolution are discussed in detail elsewhere (e.g., Aldridge et al. 2005; Chiari et al. 2008; Falkingham 2012), and on various websites (e.g., https://www.photodeler.com/kb/factors_affecting_accuracy_in_photogramm/). Our process used relatively favorable parameters (12 MP cameras, a relatively high depth of field [F8], and relatively large objects [i.e., > 10 mm]), and this promoted our ability to accurately (see definition above) reconstruct the specimens. Prior studies have shown that 3D photogrammetry is relatively accurate given basic parameters (e.g., avoidance of extreme wide-angle lenses, Aldridge et al. 2005; Chiari et al. 2008; Falkingham 2012; Postma et al. 2015; Evin et al. 2016; Amado et al. 2019; Bot and Irschick 2019), and our results are consistent with these studies. No method is “perfectly” accurate, but rather is “relatively” accurate compared to other methods.

Confirming accuracy.—Once the models were complete, we confirmed the relative accuracy of the full-body 3D meshes by comparing digital measurements of the 3D models taken in Blender software to known morphometric distances as reported in Appendices 1, 2 and 3. Morphometric measures in Appendix 1 were taken on five of the specimens that were converted to full-body 3D meshes near the time of modelling (*Dolichophis jugularis cypriacus*, *Gekko gecko*, *G. kuhli*, *Hemidactylus platyurus*, and *Stellagama stellio cypriaca*). These measures were taken with standard digital calipers accurate to 0.1 mm. For comparing on-site calipered measurements (live) with digital measurements from 3D models (digital) we used Blender software. We used linear least-squares regression to compare digital and live morphometric measurements.

RESULTS

Links to each of the five full-body 3D models and the six RAW scan models are provided in Table 1. All models are freely accessible and open to be downloaded through a creative common (CC) attribution non-commercial license. The “live” and “digital” measures were strongly correlated ($F_{1,107} = 26$; R-squared = 0.99, Y-intercept = -0.66 ± 0.27 , Slope = 1.00 ± 0.006 , $P < 0.001$). The estimated slope of 1.00 was not significantly different from an expected slope of 1.0 (if the measures were perfectly correlated, t-value = 0.17, df = 1, $P > 0.50$), which indicates that the 3D models were accurate representations of the basic shape of the living animal.

DISCUSSION

We have described devices and methods for effectively creating accurate 3D models of small live reptile and amphibian species, both in the field and the laboratory. These devices and methods can be used by field and laboratory biologists to gain valuable shape and taxonomic information on field or captive specimens. Further, as noted by others (Chiari et al. 2008;

Amado et al. 2019), 3D photogrammetry can be used to explore organismal shape in a wide range of preserved specimens, and for a variety of ecological and evolutionary purposes.

The increasingly widespread use of 3D data has provided scientists with a range of new tools that are changing how specimens are accessed, and while this approach is widely used in biology (e.g., Laforsch et al. 2012; Miller et al. 2012; Fish and Lauder 2017), the practice of 3D photocapture of living animals, and the value of such 3D models, has been less widely examined. Of course, our approach here raises the question of how these 3D models of living animals can be used in scientific applications, and how future studies can build on this framework. Prior studies have used 3D photogrammetry and modelling approaches to examine a range of questions in biology, ranging from body condition (Christiansen et al. 2019), linking body shape to climatic variables (Amado et al. 2019), to assessments of morphometric shape (Chiari et al. 2008). All these approaches remain valid for the models created using our techniques, but our focus on photocapture of living animals presents several additional possibilities. Especially for situations in which the original specimen cannot be euthanized and deposited in a natural history collection, our method may still enable species identification, which typically requires close examination of external landmarks (e.g., scales, color, morphometric variables), although genetic data represent an additional valuable source of information (Bickford et al. 2007). Indeed, our 3D modelling approach can also showcase specimens in more photogenic surroundings, such as on a leaf or piece of bark (Fig. 6; for link to the wolf snake model on bark, see <https://skfb.ly/6sFpx>). Given the trend of countries towards reducing access to collection and export of vertebrates, other means of species identification (e.g., photos, 3D models) might prove valuable in such cases.

Identifying reptile and amphibian species is multifaceted, but as an example, Watters et al. (2016) outlined key morphometric variables that are used to identify anuran species in the field. As a basic proof of concept, we were able to measure 15 of 16 of these traits on the *Polypedates* frog model (e.g., eye diameter, tympanum diameter, head width, eye–nostril distance). Only one variable (snout–vent length) could not be measured because the ventral side was hidden. That certain features were hidden during the scanning process highlights one weakness of this approach, although the fact that we were able to measure over 90% of typical species-identifying metrics suggests that these models might be used to identify most species, although more data are needed to confirm this. Conversion of the original raw 3D scans into full-body 3D meshes, such as shown here for *Dolichophis jugularis cypricus*, *Gekko gekko*, or *Stellagama stellio cyprica* offers a potential remedy to this issue, but as noted below, conversion to these full-body models is currently a time-consuming process, and using the raw 3D scans taken from a dorsal view is currently the most feasible method to scan large numbers of individuals. Furthermore, for reptile species, aspects such as scale counts in different regions represent critical information for species identification, and any full-body reconstruction would have to ensure that the integrity of scale characteristics is maintained. As a second use, as demonstrated recently by Christiansen et al. (2019), creation of 3D models of whales can be used to estimate body mass and hence body condition, which provides a valuable window into animal health. Similarly, our 3D models can be used to study volumetrics and body condition, and

then (as shown by Amado et al. 2019), related to a range of environmental variables. While measurements of body mass are typically easily gathered in the field, gathering volumetric data, or surface area data, is far more challenging, yet with basic measurement tools in open-access software such as Blender, areas and volumes are easily measured with 3D models.

A third use for our 3D models is for education and outreach regarding body shapes and colors of reptiles and amphibians. Over the past several years, integrating outreach into research programs (Ecklund et al. 2012) has become an important goal for natural history collections and scientists. These 3D models can be placed online, such as either more scientifically oriented (e.g., morphosource.org) or commercial public 3D databases (e.g., sketchfab.com), and shared widely. Most 3D viewing systems allow users on different platforms (e.g. cell phones, desktops, laptops) to manipulate, zoom in, share, and download 3D models. For example within the Digital Life Projects Sketchfab site (<https://sketchfab.com/DigitalLife3D/models>), five 3D sea turtle models created in a similar manner as the reptiles and amphibians described here (Irschick et al. 2020b) have been viewed over 80,000 times, and downloaded over 8000 times. In this manner, these 3D models also represent a valuable complement to typical vouchered specimens by providing another form of sharing data (e.g., Florida Museum of Natural History, <https://sketchfab.com/ufherps>). Further, given the growing usage of virtual and augmented reality applications (Pantelidis 2010), both at the K–12 level, and college, these 3D models provide opportunities to showcase the body shape, color, and natural history of reptiles and amphibians in a new way.

However, despite the promise of this approach, there remain several technical hurdles that need to be overcome before this system can be more widely adopted. First, for use in remote regions, our custom-made device is not an insignificant effort to transport and use. Second, 3D photogrammetry is not always effective for reconstruction of every specimen in every situation. For example, amphibians with extremely shiny skin are more challenging for photogrammetry software to reconstruct, as animals with matte-colored skin textures fare much better in the reconstruction process. As discussed in some detail by Bot and Irschick (2019), there are a number of methods to effectively reconstruct skin textures from original photographs, but such processes can be time-consuming, and are not generally amenable to a high-throughput workflow. Other considerations include the fact that not all reptiles and amphibians will stay still for the several seconds needed to photo-capture them, or they may be too elongated (e.g., snakes) to effectively view in a small space. Nevertheless, as with all new technologies and methods, there is always room for additional development and growth over time.

Acknowledgments.—We thank C. Shepard and D. McIntyre for invaluable assistance with photography. We thank J. Mendelson and R. Hill for kindly enabling us to prototype this technology. We thank A. Mukherji and C. Zeng for assistance with developing methods for organizing 3D models and photos. We thank reviewers for constructive comments on a previous version of this manuscript. The specimens in the Irschick Laboratory were photographed in accordance with an IACUC protocol approved by the University of Massachusetts at Amherst (2019-0019). All Philippine specimens were collected and photographed in accordance with the regulations established by the University of Oklahoma's Institutional Animal Care and Use Committee (IACUC

Permit Nos: R13-011 and R17-019). Field collection and export permits were provided by the Biodiversity Management Bureau (BMB) of the Philippine Department of Environment and Natural Resources (DENR) Nos. 247 and 260 (Renewal). Research on Cyprus was approved by the appropriate environmental authorities (DE – 140/4/19). Funding from an NSF grant (1353743) to C. Siler, P. Bergmann, G. Wagner, and D. Irschick supported construction of the ARRAY device. Additional funding from NSF (DEB1657648) to C. Siler and (DEB1657662) to T. Gamble and from the European Regional Development Fund and the Republic of Cyprus through the Research and Innovation Foundation (POST-DOC/0916/0034) to S. Zotos supported this research.

LITERATURE CITED

- ALICEVISION. 2018. Meshroom: A 3D reconstruction software. <https://github.com/alicevision/meshroom>
- ALLMON, W. D. 1994. The value of natural history collections. *Curator* 37:83–89.
- ALDRIDGE, K., S. A. BOYADJIEV, G. T. CAPONE, V. B. DELEON, AND J. T. RICHTSMEIER. 2005. Precision and error of three-dimensional phenotypic measures acquired from 3dMD photogrammetric images. *Am. J. Med. Gen.* 138:247–253.
- AMADO, T., M. PINTO, AND M. OLALLA-TÁRRAGA. 2019. Anuran 3D models reveal the relationship between surface area-to-volume ratio and climate. *J. Biogeogr.* 46:1429–1437.
- BICKFORD, D., D. J. LOHMAN, N. S. SODHI, P. K. L. NG, R. MEIER, K. WINKER, K. K. INGRAM, AND I. DAS. 2007. Cryptic species as a window on diversity and conservation. *Trends Ecol. Evol.* 22:148–155.
- BOT, J., AND D. J. IRSCHICK. 2019. Using 3D photogrammetry to create open-access models of live animals using open source 2D and 3D software solutions open source 2D & 3D software solutions. *In* J. Grayburn, Z. Lischer-Katz, K. Golubiewski-Davis, and V. Ikeshoji-Orlati (eds.), *3D/VR in the Academic Library: Emerging Practices and Trends*, pp. 54–72. CLIR Reports, CLIR Publication No. 176.
- BOYER, D. M., J. PUENTE, J. T. GLADMAN, C. GLYNN, S. MUKHERJEE, G. S. YAPUNCICH, AND I. DAUBECHIES. 2015. A new fully automated approach for aligning and comparing shapes. *Anat. Rec.* 298:249–276.
- CHIARI, Y., B. WANG, H. RUSHMEIER, AND A. CACCONE. 2008. Using digital images to reconstruct three-dimensional biological forms: A new tool for morphological studies. *Biol. J. Linn. Soc.* 95:425–436.
- CHRISTIANSEN, F., M. SIRONI, M. J. MOORE, M. DI MARTINO, M. RICCIARDI, H. WARICK, D. J. IRSCHICK, R. GUTIERREZ, AND M. M. UHART. 2019. Estimating body mass of free-living whales using aerial photogrammetry and 3D volumetrics. *Meth. Ecol. Evol.* 10:2034–2044.
- COMMUNITY, B. O. 2018. Blender—a 3D modelling and rendering package. Stichting Blender Foundation, Amsterdam. Retrieved from <http://www.blender.org>
- DAVIS, P. 1996. *Museums and the Natural Environment: The Role of Natural History Museums in Biological Conservation*. Leicester University Press, London. 286 pp.
- DAYRAT, B. 2005. Towards integrative taxonomy. *Biol. J. Linn. Soc.* 85:407–415.
- ECKLUND, E. H., S. A. JAMES, AND A. E. LINCOLN. 2012. How academic biologists and physicists view science outreach. *PLoS ONE* 7: e36240.
- EVIN, A., T. SOUTER, A. HULME-BEAMAN, C. AMEEN, R. ALLEN, P. VIACAVA, G. LARSON, T. CUCCHI, AND K. DOBNEY. 2016. The use of close-range photogrammetry in zooarchaeology: Creating accurate 3D models of wolf crania to study dog domestication. *J. Arch. Sci. Rep.* 9:87–93.
- FALKINGHAM, P. L. 2012. Acquisition of high resolution 3D models using free, open-source, photogrammetric software. *Palaeontol. Electron.* 15:1T:15p
- FISH, F., AND G. V. LAUDER. 2017. Control surfaces of aquatic vertebrates: active and passive design and function. *J. Exp. Biol.* 220:4351–4363.
- GIGNAC, P. M., N. J. KLEY, J. A. CLARKE, M. W. COLBERT, A. C. MORHARDT, D. CERIO, I. N. COST, P. G. COX, J. D. DAZA, C. M. EARLY, S. M. ECHOLS, M. R. HENKELMAN, A. N. HERDINA, C. M. HOLLIDAY, Z. LI, K. MAHLOW, S. MERCHANT, J. MULLER, C. ORSBON, D. J. PALUH, M. L. THIES, H. P. TSAI, AND L. M. WITMER. 2016. Diffusible iodine-based contrast-enhanced computed tomography (diceCT): An emerging tool for rapid, high-resolution, 3-D imaging of metazoan soft tissues. *J. Anat.* 228:889–909.
- GUNGA, H. C., T. SUTHAU, A. BELLMANN, A. FRIEDRICH, T. SCHWANEBECK, S. STOINSKI, T. TRIPPEL, K. KIRSCH, AND O. HELLWICH. 2007. Body mass estimations for *Plateosaurus engelhardti* using laser scanning and 3D reconstruction methods. *Naturwissenschaften* 94:623–630.
- IRSCHICK, D. J., J. MARTIN, U. SIEBERT, J. KRISTENSEN, P. T. MADSEN, AND F. CHRISTIANSEN. 2020a. Creation of accurate 3D models of harbor porpoises (*Phocoena phocoena*) using 3D photogrammetry. *Mar. Mamm. Sci.* *In review*.
- , J. BOT, A. BROOKS, M. BRESSETTE, S. FOSSETTE, A. GLEISS, R. GUTIERREZ, C. MANIRE, C. MERIGO, J. MARTIN, M. PEREIRA, S. WHITING, AND J. WYNEKEN. 2020b. Using 3D photogrammetry to create accurate 3D models of several sea turtle species as digital voucher specimens. *Herpetol. Rev.* 51:709–715.
- KÖHLER, J., M. JANSEN, A. RODRÍGUEZ, J. PHILIPPE, R. KOK, L. F. TOLEDO, M. MEERICH, F. GLAW, C. F. B. HADDAD, M. O. RÖDEL, AND M. VENCES. 2017. The use of bioacoustics in anuran taxonomy: Theory, terminology, methods and recommendations for best practice. *Zootaxa* 4251:1–124.
- LAFORSCH, C., H. IMHOF, S. ROBERT, M. SETTLES, AND M. W. A. HEB. 2012. Applications of computational 3D-modeling in organismal biology. *In* D. J. Murray-Smith (ed.), *Modeling and Simulation in Engineering Sciences*, pp. 117–142. Woodhead Publishing, Cambridge, UK.
- MCDIARMID, R. W., M. S. FOSTER, C. GUYER, J. W. GIBBONS, AND N. CHERNOFF (eds.). 2011. *Reptile Biodiversity: Standard Methods for Inventory and Monitoring*. University of California Press, Berkeley, California. 424 pp.
- MILLER, L. A., D. I. GOLDMAN, T. L. HEDRICK, E. D. TYTELL, Z. J. WANG, J. YEN, AND S. ALBEN. 2012. Using computational models to study animal locomotion. *Integr. Comp. Biol.* 52:553–575.
- PANTELIDIS, V. S. 2010. Reasons to use virtual reality in education and training courses and a model to determine when to use virtual reality. *Themes in Science and Technology Education Special Issue, Klidarithmos Computer Books*, pp. 59–70.
- POSTMA, M., A. S. W. TORDIFFE, M. S. HOFMEYER, R. R. REISINGER, L. C. BESTER, P. E. BUSS, AND P. J. N. DE BRUYN. 2015. Terrestrial mammal three-dimensional photogrammetry: Multispecies mass estimation. *Ecosphere* 6:1–16.
- RENNER, S. C., D. NEUMANN, M. BURKART, U. FEIT, P. GIERE, A. PAULSCH, C. PAULSCH, M. STERZ, C. HAUSER, AND K. VOHLAND. 2012. Import and export of biological samples from tropical countries—considerations and guidelines for research teams. *Organisms, Diversity and Evolution* 12:81–98.
- REYNOLDS, R., AND R. W. MCDIARMID. 2011. Voucher specimens. *In* R. W. McDiarmid, M. S. Foster, C. Guyer, J. W. Gibbons, and N. Chernoff (eds.), *Reptile Biodiversity: Standard Methods for Inventory and Monitoring*, pp. 87–94. University of California Press, Berkeley, California.
- SCHÖNBERGER, J. L., AND J.-M. FRAHM. 2016. Structure-from-Motion revisited. *Proceedings of the IEEE Conference on Computer Vision and Pattern Recognition (CVPR)*, pp. 4104–4113. Las Vegas, Nevada.
- SHAFFER, H. B., R. N. FISHER, AND C. DAVIDSON. 1998. The role of natural history collections in documenting species declines. *Trends Ecol. Evol.* 13:27–30.
- SIMMONS, J. E. 2015. *Herpetological Collecting and Collections Management*. Society for the Study of Amphibians and Reptiles Herpetological Circular No. 42. 191 pp.

- SUAREZ, A. V., AND N. D. TSUTSUI. 2004. The value of museum collections for research and society. *Bioscience* 54:66–74.
- WEINBERG, S. M., N. M. SCOTT, K. NEISWANGER, C. A. BRANDON, AND M. L. MARAZITA. 2004. Digital three-dimensional photogrammetry: Evaluation of anthropometric precision and accuracy using a Genex 3D camera system. *Cleft-Palate Craniofac. J.* 41:507–518.
- WATTERS, J. L., S. T. CUMINGS, R. L. FLANAGAN, AND C. D. SILER. 2016. Review of morphometric measurements used in anuran species descriptions and recommendations for a standardized approach. *Zootaxa* 4072:477–495.

APPENDIX 1

Morphometric measurements taken on several of the species sampled to test for accuracy of the 3D models.

Gekko gekko, *G. kuhli*, *Hemidactylus platyurus*, *Stellagama stellio cyprica*: total length (distance between tip of nose to tip of tail); snout–vent length (distance between tip of nose to cloaca from the ventral side); body length (distance between cloaca to insertion of head into the shoulder); Forelimb to hindlimb distance (distance between the primary fore-limb joint to the primary hind limb joint when both limbs are held in a natural posture); head length (distance between insertion of the head and tip of nose); head width (greatest width of the head as measured close to the

ear); head depth (greatest depth of the head, as typically measured in front of the ear); body width (width of the body from side to side as taken at the mid-point of the body); pelvic width (distance between the insertion of each limb at the pelvis); tail width (maximum width of the tail as measured from side to side, typically measured near the cloaca); pelvic height (maximum height of the pelvis, typically measured in front of the cloaca); Humerus length (an estimated length of the humerus, taken from insertion of the limb into the body to the elbow joint); Ulna length (an estimated length of the ulna, taken from primary elbow joint to insertion of toes); Forefoot length (an estimate of metacarpal length on the forefoot, taken from tip of longest toe to insertion of toe into foot); Femur length (an estimate of femur length, taken from insertion of the limb into the body and the knee joint); Tibia length (an estimate of tibia length, taken from knee joint to insertion of limb into body); Hindfoot (an estimate of the metacarpal length on the hindfoot, taken from the edge of the heel to the tip of the longest toe). *Dolichophis jugularis*: tail length (distance between tip of tail and cloaca); total length (distance between tip of tail and tip of nose); head width (same measure as above); head length (same measure as above); head length (same measure as above); head depth (same measure as above, circumference every 10 cm from tip of nose to tip of tail (18 measurements)); body depth (distance from dorsal to ventral side of body) taken every 10 cm from tip of nose to tip of tail (18 measurements).

APPENDIX 2

Morphometric data for the four lizard species. Values in cm.

	<i>Gekko gekko</i>	<i>Gekko kuhli</i>	<i>Hemidactylus platyurus</i>	<i>Stellagama stellio cyprica</i>
Total length	265.0	165.0	92.0	19.4
Snout–vent length	144.0	85.0	53.0	10.7
Body length	86.0	75.0	36.0	6.8
Forelimb to hindlimb distance	73.0	49.0	24.5	4.2
Head length	54.0	38.0	14.5	2.7
Head width	37.0	22.0	11.0	2.8
Head depth	29.0	10.0	7.0	1.8
Body width	43.0	21.0	12.5	3.0
Pelvic width	18.0	10.1	8.5	1.8
Tail width	15.0	17.0	6.5	1.7
Pelvic height	20.0	8.5	4.5	1.4
Humerus Length	27.0	10.5	7.0	1.9
Ulna Length	26.0	9.0	8.5	2.3
Forefoot Length	17.0	11.0	6.5	1.6
Femur Length	24.0	18.0	9.5	2.3
Tibia Length	29.0	14.5	9.0	3.0
Hindfoot Length	26.0	14.0	8.0	3.1

APPENDIX 3

Morphometric data from the snake specimen *Dolichophis jugularis*. Values in cm

Variable	<i>Dolichophis jugularis</i>
Tail length	43.0
Total length	189.0
Head width	1.6
Head length - 1	1.7
Head length - 2	3.1
Head depth	1.5
Circumference 10 cm	5.2
Circumference 20 cm	6.7
Circumference 30 cm	7.6
Circumference 40 cm	7.7
Circumference 50 cm	7.7
Circumference 60 cm	8.1
Circumference 70 cm	8.7
Circumference 80 cm	8.2
Circumference 90 cm	7.5
Circumference 100 cm	7.0
Circumference 110 cm	6.8
Circumference 120 cm	6.8
Circumference 130 cm	6.8
Circumference 140 cm	6.2
Circumference 150 cm	4.8
Circumference 160 cm	4.0
Circumference 170 cm	3.2
Circumference 180 cm	2.1
Depth 10 cm	1.9
Depth 20 cm	2.4
Depth 30 cm	2.7
Depth 40 cm	3.1
Depth 50 cm	3.3
Depth 60 cm	3.2
Depth 70 cm	3.2
Depth 80 cm	3.1
Depth 90 cm	2.8
Depth 100 cm	2.8
Depth 110 cm	2.5
Depth 120 cm	2.5
Depth 130 cm	2.5
Depth 140 cm	2.2
Depth 150 cm	1.6
Depth 160 cm	1.4
Depth 170 cm	1.0
Depth 180 cm	0.6